Controlling a Subdivision Tuning Method

Ingo Ginkel and Georg Umlauf

Abstract. In this paper the problem of curvature behavior around extraordinary points of a Loop subdivision surface is addressed. For subdivision surfaces, configurations of the initial control net exist in which neither the elliptic nor the hyperbolic component of the initial control net becomes dominant. This leads to so-called hybrid shapes which often cause visible artifacts. A solution to this problem is to split it into two parts: first an eigenvalue tuning to allow for bounded Gauss curvature with arbitrary sign and, second, an eigencoefficient tuning to avoid hybrid shapes. The techniques for eigencoefficient tuning will now be analyzed in detail. The analysis allows to quantify the difference between the original and the modified surfaces. Additionally, extensions to the eigencoefficient tuning techniques are given to solve various problems that might be imposed by the topology of the initial control net.

§1. Introduction

Tuning has always been part of developing subdivision algorithms. The choice of suitable parameters for the first algorithms [3, 7] already improved the shape of the surfaces. The next step was eigenvalue tuning in the frequency domain to achieve zero or bounded curvature[13, 6, 11, 8, 9]. Recently, more sophisticated approaches that focus on shape improvement were made. Eigenvector optimization is used to approximate C^2-conditions in [2]. The number of so-called hybrid shapes is decreased by eigenvalue tuning to minimize the variation of Gauss curvature near extraordinary points in [1].

In [4] it was shown how hybrid shapes can be avoided. The solution consists of two steps. First, an eigenvalue tuning is used to allow for surfaces with bounded Gauss curvature of arbitrary sign. Second, two alternative methods for tuning the eigencoefficients of the initial control net can be used to achieve an elliptic or a hyperbolic shape at the extraordinary points.

The rest of this paper is structured as follows. §2 recalls the basic principles of analyzing subdivision algorithms following [12, 10]. Using a variant of the algorithm of Loop generating surfaces with bounded Gauss curvature of arbitrary sign (BCLSS), §3 describes and analyzes the symmetric eigencoefficient tuning technique to avoid hybrid shapes ([4]). A local optimization technique to avoid hybrid shapes ([4]) with different extensions is presented and analyzed in §4. Here, we address problems that might be imposed by the topology of the initial control net.

§2. Analyzing Subdivision Algorithms

We consider a subdivision surface $\mathbf{x}$ generated by a stationary, linear and symmetric subdivision algorithm generalizing box spline subdivision. This allows to make use of the standard analysis techniques [12, 10].

In the neighborhood of an irregular vertex of valence $n \neq 6$ of a triangular net a subdivision surface can be regarded as the union of the extraordinary point $\mathbf{m}$ and a sequence of spline rings $\mathbf{x}_m$. A spline ring is a linear combination of real valued functions $\varphi_0(s,t), \ldots, \varphi_L(s,t)$ with control points $\mathbf{B}_m^0, \ldots, \mathbf{B}_m^L \in \mathbb{R}^3$. Collecting the functions in a row vector $\boldsymbol{\varphi}(s,t)$ and the control points in a column vector $\mathbf{B}_m$ yields $\mathbf{x}_m = \boldsymbol{\varphi}\mathbf{B}_m = \boldsymbol{\varphi}A^m\mathbf{B}_0$, where the sequence of control nets $\mathbf{B}_m$ is generated by iterated application of a square subdivision matrix A to the initial control net $\mathbf{B}_0$. The subdivision matrix A has eigenvalues $\lambda_0, \ldots, \lambda_L$ with $|\lambda_0| \geq |\lambda_1| \geq \cdots \geq |\lambda_L|$, corresponding to right eigenvectors $\mathbf{v}_0, \ldots, \mathbf{v}_L$, and eigenfunctions $\psi_i(s,t) = \boldsymbol{\varphi}(s,t)\mathbf{v}_i$, which are the limit functions of $\mathbf{v}_i$ under box spline subdivision. The special spline ring $\boldsymbol{\Psi}(s,t) := (\psi_1(s,t), \psi_2(s,t))$ is called the characteristic map. The initial control net can be written as $\mathbf{B}_0 = \sum_{i=0}^{L} \mathbf{d}_i \mathbf{v}_i$ and we assume that the $\mathbf{d}_i$ are generic as defined in [10].

There are well-known sufficient conditions on the eigenvalues and eigenvectors to ensure convergence, C^1 regularity, bounded curvature and allow for arbitrary quadratic shapes [12]. Unfortunately the standard algorithms, e.g. the algorithm of Loop, do not meet these conditions and must be modified. Therefore, we assume for the rest of this paper a subdivision algorithm based on the algorithm of Loop modified to generate subdivision surfaces with bounded Gauss curvature of arbitrary sign, called for short B(ounded)C(urvature)L(oop)S(ubdivision)S(cheme). We assume that a BCLSS has eigenvectors with the same structure as the eigenvectors of the algorithm of Loop. An example for a BCLSS is given in [4].

To analyze the curvature behavior of a subdivision algorithm, the central surface is defined as the spline ring

$$\mathbf{x}_c := \big(\boldsymbol{\Psi}L, \psi_3\langle\mathbf{d}_3, \mathbf{n}\rangle + \psi_4\langle\mathbf{d}_4, \mathbf{n}\rangle + \psi_5\langle\mathbf{d}_5, \mathbf{n}\rangle\big), \ \mathbf{n} := (\mathbf{d}_1 \times \mathbf{d}_2)/\|\mathbf{d}_1 \times \mathbf{d}_2\|,$$

where L is the matrix orthonormalizing $(\mathbf{d}_1, \mathbf{d}_2)$. The Gauss curvature $K_{\mathbf{x}_c}$ of $\mathbf{x}_c$ can be used to classify the behavior of the Gauss curvature of

x at an extraordinary point **m** a priori [10]:

$$\mathbf{m} \text{ is } \begin{cases} \text{elliptic in the limit,} & \text{if } K_{\mathbf{x}_c}(s,t) > 0 \text{ for all } s,t, \\ \text{hyperbolic in the limit,} & \text{if } K_{\mathbf{x}_c}(s,t) < 0 \text{ for all } s,t, \\ \text{hybrid,} & \text{otherwise.} \end{cases}$$

Furthermore, for every **m** the shape category can be pre-computed. The third coordinate of $\mathbf{x}_c$ can be written in polar coordinates as

$$\sum_{i=3}^{5} \psi_i \langle \mathbf{d}_i, \mathbf{n} \rangle = (1-r)\psi_3 + r\cos(\vartheta)\psi_4 + r\sin(\vartheta)\psi_5,$$

where $r \in [0,1]$ and $\vartheta \in [0,2\pi]$. Without loss of generality this allows only for $\mathbf{d}_3$ pointing in the direction of **n**. This is achieved by

$$r = \frac{\sqrt{\langle \mathbf{d}_4, \mathbf{n} \rangle^2 + \langle \mathbf{d}_5, \mathbf{n} \rangle^2}}{\sqrt{\langle \mathbf{d}_4, \mathbf{n} \rangle^2 + \langle \mathbf{d}_5, \mathbf{n} \rangle^2 + \langle \mathbf{d}_3, \mathbf{n} \rangle}}, \qquad \vartheta = \arccos \frac{\langle \mathbf{d}_4, \mathbf{n} \rangle}{\sqrt{\langle \mathbf{d}_4, \mathbf{n} \rangle^2 + \langle \mathbf{d}_5, \mathbf{n} \rangle^2}}.$$

Denote by $K_{r,\vartheta}(s,t)$ the Gauss curvature of $\mathbf{x}_c$ defined by (r,ϑ) at the parameter (s,t). Then, the *shape chart map* **s** is defined by

$$\mathbf{s}(r,\vartheta) = \begin{cases} 0, & \text{if } K_{r,\vartheta}(s,t) < 0 \text{ for all } s,t, \\ 1, & \text{if } K_{r,\vartheta}(s,t) > 0 \text{ for all } s,t, \\ \frac{1}{2}, & \text{otherwise.} \end{cases}$$

The mapping of $\mathbf{s}(r,\vartheta)$ to the colors blue, green and red yields the so-called *shape chart*. More details on shape charts can be found in [10, 5].

§3. A Symmetric Technique to Avoid Hybrid Shapes

Given a BCLSS changing the position of the central vertex only affects the eigencoefficients $\mathbf{d}_0$ and $\mathbf{d}_3$. So, scaling $\mathbf{d}_3$ by α can be written as a symmetric averaging stencil applied to the central vertex as shown in Figure 1, where $\alpha > 1$ corrects the shape to an elliptic and $\alpha < 1$ to a hyperbolic shape. This technique is summarized by the algorithm $S_{a,b}$:

1. Subdivide the control net with the BCLSS once.
2. Decide if the eigencoefficients $\mathbf{d}_3$, $\mathbf{d}_4$, $\mathbf{d}_5$ represent a hybrid shape [4].
3. Subdivide the control net a times with the BCLSS.
4. If $\mathbf{d}_3$, $\mathbf{d}_4$, $\mathbf{d}_5$ represent a hybrid shape and $b > 0$, use the correction stencil in Figure 1 once.
5. Steps 1. and 4. are repeated $b-1$ times.
6. Subdivide the control net with the BCLSS.

Note that $S_{0,0}$ represents the usual BCLSS. The parameter a delays the correction by $a+1$ iteration steps. The parameter b decelerates the correction to reduce the difference between the original and the corrected surface. The choice of α, a and b will be discussed in the sequel.

Fig. 1. The stencil for the correction.
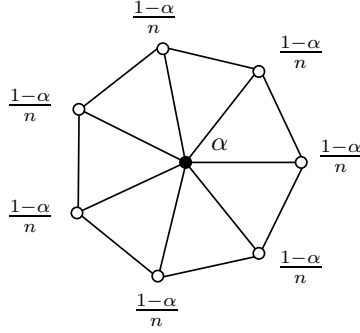
3.1. Choosing α without shape charts

To simplify Step 2. of $S_{a,b}$, use bounds $r_{\min}$ so that $r < r_{\min}$ produce elliptic shapes and $r_{\max}$ so that $r > r_{\max}$ produce hyperbolic shapes. This implies bounds for α without using the shape charts. To compute r after Step 4., $(\alpha \cdot \langle \mathbf{d}_3, \mathbf{n} \rangle, \langle \mathbf{d}_4, \mathbf{n} \rangle, \langle \mathbf{d}_5, \mathbf{n} \rangle)$ is transformed to polar coordinates

$$r = \frac{\sqrt{\langle \mathbf{d}_4, \mathbf{n} \rangle^2 + \langle \mathbf{d}_5, \mathbf{n} \rangle^2}}{\sqrt{\langle \mathbf{d}_4, \mathbf{n} \rangle^2 + \langle \mathbf{d}_5, \mathbf{n} \rangle^2} + \alpha \langle \mathbf{d}_3, \mathbf{n} \rangle}.$$

To guaranteed the desired shape after the correction, use the bounds

$$\alpha > \frac{\sqrt{\langle \mathbf{d}_4, \mathbf{n} \rangle^2 + \langle \mathbf{d}_5, \mathbf{n} \rangle^2}(1 - r_{\min})}{r_{\min} \langle \mathbf{d}_3, \mathbf{n} \rangle}, \qquad \text{for an elliptic shape,}$$

$$\alpha < \frac{\sqrt{\langle \mathbf{d}_4, \mathbf{n} \rangle^2 + \langle \mathbf{d}_5, \mathbf{n} \rangle^2}(1 - r_{\max})}{r_{\max} \langle \mathbf{d}_3, \mathbf{n} \rangle}, \qquad \text{for a hyperbolic shape.}$$

Assuming the right eigenvectors $\mathbf{v}_i$ and left eigenvectors $\mathbf{w}_i$ to be scaled such that $\|\mathbf{v}_i\| = 1 = \mathbf{w}_i \mathbf{v}_i$, bounds $r_{\min}$ and $r_{\max}$ for the BCLSS of [4] are given in Table 1 for $n = 5, \ldots, 14$.

n	$r_{\min}$	$r_{\max}$	n	$r_{\min}$	$r_{\max}$	n	$r_{\min}$	$r_{\max}$
5	0.403	0.485	9	0.368	0.492	12	0.326	0.562
7	0.404	0.455	10	0.353	0.513	13	0.313	0.593
8	0.385	0.474	11	0.339	0.536	14	0.301	0.631

Tab. 1. Bounds $r_{\min}$ and $r_{\max}$ for the BCLSS of [4].

3.2. Comparing the uncorrected and the corrected surface

The limit point $\mathbf{d}_0$ can be computed using the left eigenvector $\mathbf{w}_0$. Denote by $\mathbf{d}_i^{a,b}(\mathbf{p})$ the eigencoefficient of $\mathbf{v}_i$ corresponding to a vertex $\mathbf{p}$ after Step 5. of $S_{a,b}$. For a vertex $\mathbf{p}_0$ and its one-ring neighborhood $\mathbf{p}_1, \ldots, \mathbf{p}_n$

$$\mathbf{d}_0^{0,0}(\mathbf{p}_0) = \kappa \cdot \sum_{i=1}^n \mathbf{p}_i + (1 - n\kappa) \cdot \mathbf{p}_0, \qquad \text{with } \kappa := (3/(8\beta) + n)^{-1},$$

$$\mathbf{d}_0^{0,1}(\mathbf{p}_0) = \kappa \cdot \sum_{1=1}^{n} \mathbf{p}_i + (1 - n\kappa) \cdot \frac{1-\alpha}{n} \sum_{1=1}^{n} \mathbf{p}_i + \alpha\mathbf{p}_0.$$

So the difference between these limit points is

$$
\begin{aligned}
\mathbf{d}_0^{0,0}(\mathbf{p}_0) - \mathbf{d}_0^{0,1}(\mathbf{p}_0) &= (1 - n\kappa)(1 - \alpha)\left(\mathbf{p}_0 - \frac{1}{n}\sum_{i=1}^{n}\mathbf{p}_i\right) \\
&= -(1 - n\kappa)(1 - \alpha) \cdot \mathbf{d}_3^{0,0}(\mathbf{p}_0).
\end{aligned}
$$

Since subdivision scales the eigencoefficients, this generalizes to

$$\mathbf{d}_0^{a,0}(\mathbf{p}_0) - \mathbf{d}_0^{a,1}(\mathbf{p}_0) = -\mu^a(1 - n\kappa)(1 - \alpha) \cdot \mathbf{d}_3^{0,0}(\mathbf{p}_0).$$

Analogously, we can compute the difference of the surfaces at points corresponding to the vertices $\mathbf{p}_i$ of the one-ring neighborhood of $\mathbf{p}_0$, i.e.

$$\mathbf{d}_0^{0,0}(\mathbf{p}_i) - \mathbf{d}_0^{0,1}(\mathbf{p}_i) = -(1 - \alpha) \cdot \mathbf{d}_3^{0,0}(\mathbf{p}_0)/12, \quad i = 1, \ldots, n.$$

Since $1 - n\kappa > 1/12$ for $n > 6$, the difference between the surfaces is largest at the extraordinary point. Thus, it is possible to control the error. Given a tolerance ε and a correction factor α, solve $\mu^a(1 - n\kappa)(1 - \alpha)\|\mathbf{d}_3\| < \varepsilon$ for a. So, to guarantee the tolerance ε at $\mathbf{m}$ for $S_{a,1}$ chose a as

$$a > \log_\mu\left(\varepsilon/((1 - n\kappa)(1 - \alpha)\|\mathbf{d}_3\|)\right).$$

To analyze the effect of b subdivision and correction steps, observe that $\mathbf{d}_3^{a,b} = \mu^a \mathbf{d}_3^{0,b}$ and $\mathbf{d}_3^{a,b} = \mu^b \alpha^b \mathbf{d}_3^{a,0}$. This yields $\mathbf{d}_3^{a,b} = \mu^{a+b}\alpha^b \mathbf{d}_3^{0,0}$. The difference between the points $\mathbf{d}_0^{a,0}(\mathbf{p}_0)$ and $\mathbf{d}_0^{a,b}(\mathbf{p}_0)$ is a telescoping sum

$$
\begin{aligned}
\mathbf{d}_0^{a,0} - \mathbf{d}_0^{a,b} &= -\mu^a(1 - n\kappa)(1 - \alpha)\sum_{i=0}^{b-1}\mathbf{d}_3^{0,i} \\
&= -\mu^a(1 - n\kappa)(1 - \alpha)\frac{(\alpha\mu)^b - 1}{\alpha\mu - 1} \cdot \mathbf{d}_3^{0,0},
\end{aligned}
$$

where we skipped the argument $\mathbf{p}_0$ for simplicity. This allows to control the difference between the limit surfaces of the BCLSS and $S_{a,b}$.

An example for the application of this technique to a large initial control net is shown in Figure 2. Note that still some artifact is visible in the zoom picture of the corrected vertex, although hyperbolic shape in the limit is guaranteed. This motivates the use of conservative bounds causing a larger correction than theoretically necessary.

§4. A Local Optimization Technique to Avoid Hybrid Shapes

The local optimization technique for a BCLSS in [4] gives more control over the surface away from extraordinary points. First we recall this technique for isolated irregular vertices and then present improvements of the optimization and extensions to close irregular vertices.
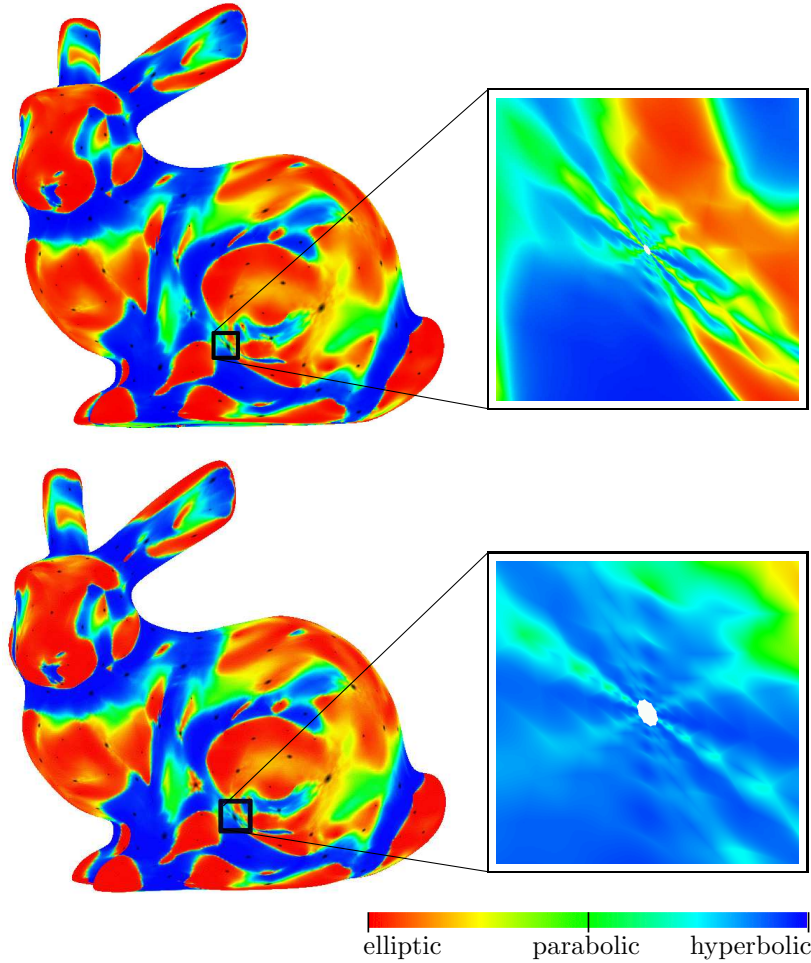
Fig. 2. Bunny with 566 vertices, 15 vertices correspond to points on the surface with hybrid shape (top row), 7 vertices were corrected to elliptic and 8 vertices to hyperbolic behavior (bottom row). For color images please refer to our website.

4.1. The basic technique

The coefficients $\mathbf{d}_k$, $k = 1, \ldots, 5$, can be computed using the corresponding left row eigenvectors $\mathbf{w}_k$ and the central vertex $\mathbf{p}_0$ and its one-ring neighborhood $\mathbf{p}_1, \ldots, \mathbf{p}_n$. So, the $\mathbf{d}_k$ can be computed as

$$\mathbf{d} := [\mathbf{d}_0 \ldots \mathbf{d}_5]^T = [\mathbf{w}_0^T \ldots \mathbf{w}_5^T]^T \cdot [\mathbf{p}_0 \ldots \mathbf{p}_n]^T =: W_n \cdot \mathbf{p}.$$

This has an exact solution for $n = 5$, and is under-determined for $n > 5$.

If the coefficients $\mathbf{d}_k$ represent a hybrid shape, change $\mathbf{d}_3$, $\mathbf{d}_4$ and $\mathbf{d}_5$ to

$$\mathbf{d}_3' = \mathbf{d}_3 + \kappa_3 \cdot \mathbf{n}, \quad \mathbf{d}_4' = \mathbf{d}_4 + \kappa_4 \cdot \mathbf{n}, \quad \mathbf{d}_5' = \mathbf{d}_5 + \kappa_5 \cdot \mathbf{n}$$

such that $\langle \mathbf{d}_3', \mathbf{n} \rangle$, $\langle \mathbf{d}_4', \mathbf{n} \rangle$ and $\langle \mathbf{d}_5', \mathbf{n} \rangle$ generate a non-hybrid surface using [4]. Now, the system of equations is changed to $W_n \cdot \mathbf{p}' = \mathbf{d}'$ with $\mathbf{d}' := [\mathbf{d}_0, \mathbf{d}_1, \mathbf{d}_2, \mathbf{d}_3', \mathbf{d}_4', \mathbf{d}_5']^T$. If W_n^+ is the Moore-Penrose inverse of W_n, then

$$\mathbf{p}' = \mathbf{p} + W_n^+(\mathbf{d}' - W_n \cdot \mathbf{p})$$

yields control points which solve $W_n \cdot \mathbf{p}' = \mathbf{d}'$ and minimize $\sum_i \|\mathbf{p}_i' - \mathbf{p}_i\|^2$. Replacing $\mathbf{p}$ with $\mathbf{p}'$ subdivision results in a surface with the same limit point $\mathbf{d}_0$, the same tangent directions $\mathbf{d}_1$ and $\mathbf{d}_2$, but avoids hybrid shapes.

4.2. Improving the local optimization

So far only modifications of the normal components of the $\mathbf{d}_i$, $i = 3, 4, 5$, have been considered. This means that the differences between the old $\mathbf{p}$ and new control points $\mathbf{p}'$ are only in the normal direction, because

$$
\begin{aligned}
\mathbf{p}' - \mathbf{p} &= W_n^+(\mathbf{d}' - W_n \cdot \mathbf{p}) = W_n^+(\mathbf{d}' - \mathbf{d}) = W_n^+(\mathbf{d} + \boldsymbol{\kappa} \cdot \mathbf{n}^T - \mathbf{d}) \\
&= W_n^+ \cdot \boldsymbol{\kappa} \cdot \mathbf{n}^T, \qquad \text{where } \boldsymbol{\kappa} := [0, 0, 0, \kappa_3, \kappa_4, \kappa_5]^T.
\end{aligned}
$$

Adding tangential components to the optimization might decrease $\|\mathbf{p}' - \mathbf{p}\|^2$, because this does not change the shape chart classification. Repeating the above computation for new points $\widetilde{\mathbf{p}}'$ with $\mathbf{d}' = \mathbf{d} + \boldsymbol{\kappa}\mathbf{n}^T + \boldsymbol{\alpha}\mathbf{d}_1^T + \boldsymbol{\beta}\mathbf{d}_2^T$ yields for $\boldsymbol{\alpha} := [0, 0, 0, \alpha_3, \alpha_4, \alpha_5]^T$ and $\boldsymbol{\beta} := [0, 0, 0, \beta_3, \beta_4, \beta_5]^T$

$$\widetilde{\mathbf{p}}' - \mathbf{p} = W_n^+(\boldsymbol{\kappa}\mathbf{n}^T + \boldsymbol{\alpha}\mathbf{d}_1^T + \boldsymbol{\beta}\mathbf{d}_2^T).$$

Thus, $\|\widetilde{\mathbf{p}}_i' - \mathbf{p}_i\| \geq \|\mathbf{p}_i' - \mathbf{p}_i\|$ for all i, since the normal component $\boldsymbol{\kappa}\mathbf{n}$ must not change and $\mathbf{n} \perp \mathbf{d}_1, \mathbf{d}_2$. So, tangential changes do not improve the optimization. Also changes of $\mathbf{d}_1$ and $\mathbf{d}_2$ do not improve the optimization.

A way to decrease $\|\mathbf{p}' - \mathbf{p}\|^2$ is to scale $\langle \mathbf{d}_i, \mathbf{n} \rangle \mathbf{n}$, $i = 3, 4, 5$, by the same factor α, since this also does not change the shape chart classification. With $\boldsymbol{\lambda} = [0, 0, 0, \langle \mathbf{d}_3, \mathbf{n} \rangle, \langle \mathbf{d}_4, \mathbf{n} \rangle, \langle \mathbf{d}_5, \mathbf{n} \rangle]^T$ we set $\mathbf{d}'$ to $\widetilde{\mathbf{d}}' := \mathbf{d} + \boldsymbol{\kappa}\mathbf{n}^T + \alpha\boldsymbol{\lambda}\mathbf{n}^T$ and find for the distance of the old $\mathbf{p}$ and new control points $\widetilde{\mathbf{p}}'$

$$\|\widetilde{\mathbf{p}}' - \mathbf{p}\|^2 = \|\mathbf{p}' - \mathbf{p} + \alpha W_n^+ \boldsymbol{\lambda}\mathbf{n}^T\|^2 = \sum_{i=0}^{n} \sum_{j=1}^{3} \left(\mathbf{p}_{ij}' - \mathbf{p}_{ij} + \alpha w_{ij}\right)^2,$$

where the additional index j denotes the j-th coordinate of the respective points and $W_n^+ \boldsymbol{\lambda}\mathbf{n}^T =: [w_{ij}]_{i,j}$. Differentiation with respect to α yields

$$\frac{\partial}{\partial \alpha}\|\widetilde{\mathbf{p}}' - \mathbf{p}\|^2 = 2 \sum_{i=0}^{n} \sum_{j=1}^{3} (\mathbf{p}_{ij}' - \mathbf{p}_{ij} + \alpha w_{ij}) w_{ij},$$

which vanishes if and only if

$$\alpha = \left(\sum_{i=0}^{n} \sum_{j=1}^{3} (\mathbf{p}_{ij} - \mathbf{p}'_{ij}) w_{ij} \right) \left(\sum_{i=0}^{n} w_{ij}^2 \right)^{-1}.$$

This choice of α will further decrease the distance between the old and new control points without changing the shape chart classification.

4.3. Irregular vertices with overlapping neighborhood

For separated irregular vertices, each system of equations can be solved separately. This is not possible, if the neighborhoods overlap.

Denote by $\mathbf{p}_0$ and $\mathbf{q}_0$ two irregular vertices with valence n_1 and n_2 that share a vertex in their one-ring neighborhoods $\mathbf{p}_1, \dots, \mathbf{p}_{n_1}$ and $\mathbf{q}_1, \dots, \mathbf{q}_{n_2}$ such that $\mathbf{p}_k = \mathbf{q}_l$, for one $k \in \{1, \dots, n_1\}$ and $l \in \{1, \dots, n_2\}$. Denote by $\mathbf{d}_j^p$ and $\mathbf{d}_j^q$, $j = 0, \dots, 5$, the associated eigencoefficients for $\mathbf{p}_0$ and $\mathbf{q}_0$. Computing the new control points for each neighborhood as in §4.2 will in general give different solutions $\widetilde{\mathbf{p}}_k \neq \widetilde{\mathbf{q}}_l$ for the new position of $\mathbf{p}_k = \mathbf{q}_l$. Since the systems of equations are under-determined for $n > 5$, we average the positions $\overline{\mathbf{p}}_k = (\widetilde{\mathbf{p}}_k + \widetilde{\mathbf{q}}_k)/2$ and change the systems of equations to

$$\begin{aligned} W_{n_1}^k \cdot \mathbf{p} &= [\mathbf{d}_0^p, \mathbf{d}_1^p, \mathbf{d}_2^p, \mathbf{d}_3'^p, \mathbf{d}_4'^p, \mathbf{d}_5'^p, \overline{\mathbf{p}}_k]^T, \\ W_{n_2}^l \cdot \mathbf{q} &= [\mathbf{d}_0^q, \mathbf{d}_1^q, \mathbf{d}_2^q, \mathbf{d}_3'^q, \mathbf{d}_4'^q, \mathbf{d}_5'^q, \overline{\mathbf{p}}_k]^T, \end{aligned}$$

with $\mathbf{p} := [\mathbf{p}_0 \dots \mathbf{p}_{n_1}]^T$, $\mathbf{q} := [\mathbf{q}_0, \mathbf{q}_1, \dots, \mathbf{q}_{n_2}]^T$ and $W_{n_1}^k$ extends W_{n_1} by the k-th unit row vector $[0, \dots 0, 1, 0, \dots, 0]$, $W_{n_2}^l$ analogously. Solving these systems gives a unique new position for the shared vertex. This technique can be used for $\min(n_1, n_2) - 5$ shared points.

This technique can be extended to allow vertices with valence 5. If $n_1 = 5$ and $n_2 > 5$, we can set the first and second system of equations to

$$\begin{aligned} W_5 \cdot \mathbf{p} &= [\mathbf{d}_0^p, \mathbf{d}_1^p, \mathbf{d}_2^p, \mathbf{d}_3'^p, \mathbf{d}_4'^p, \mathbf{d}_5'^p]^T, \\ W_{n_2}^l \cdot \mathbf{q} &= [\mathbf{d}_0^q, \mathbf{d}_1^q, \mathbf{d}_2^q, \mathbf{d}_3'^q, \mathbf{d}_4'^q, \mathbf{d}_5'^q, \widetilde{\mathbf{p}}_k]^T, \end{aligned}$$

which will also give a solution with a unique new position $\widetilde{\mathbf{p}}_k$ for the shared vertex. If $n_1 = n_2 = 5$, a possible solution for a single shared vertex is

$$\begin{aligned} \widetilde{W}_5^k \cdot \mathbf{p} &= [\mathbf{d}_1^p, \mathbf{d}_2^p, \mathbf{d}_3'^p, \mathbf{d}_4'^p, \mathbf{d}_5'^p, \overline{\mathbf{p}}_k]^T, \\ \widetilde{W}_5^l \cdot \mathbf{q} & \quad [\mathbf{d}_1^q, \mathbf{d}_2^q, \mathbf{d}_3'^q, \mathbf{d}_4'^q, \mathbf{d}_5'^q, \overline{\mathbf{p}}_k]^T, \end{aligned}$$

where $\widetilde{W}_n^k$ is W_n^k without the first row. This will also give a unique new position $\overline{\mathbf{p}}_k$ for the shared vertex, but modified limit positions $\mathbf{d}_0^p$ and $\mathbf{d}_0^q$.

To summarize, this technique allows the treatment of irregular vertices with overlapping one-ring neighborhood but cannot be applied to adjacent irregular vertices. Example surfaces are shown in Figure 3.
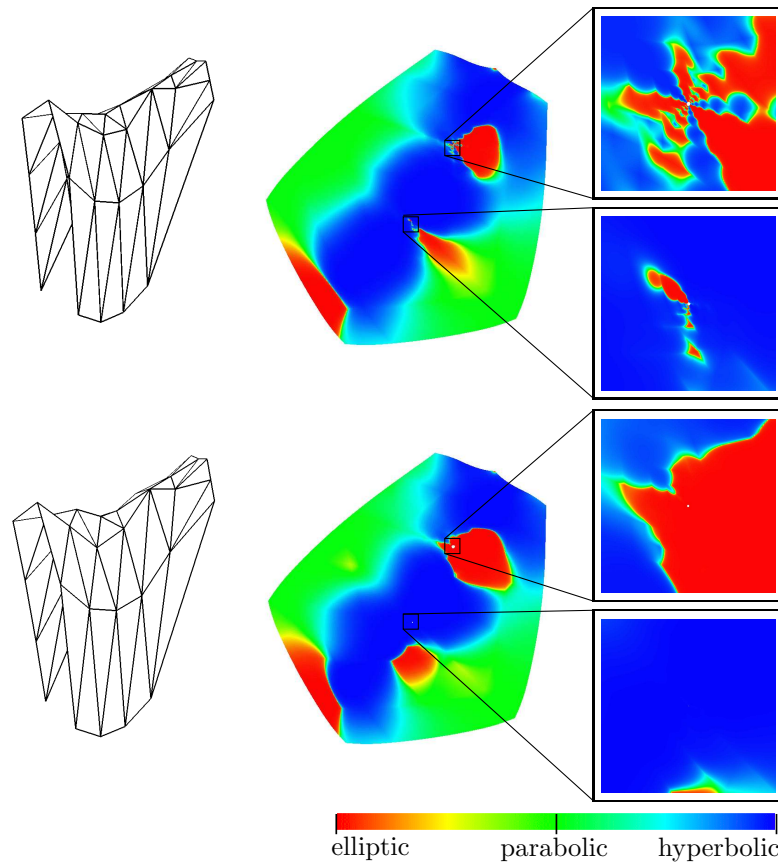
Fig. 3. The Gauss curvature (middle, zoom right) of the limit surface for a control net (left) with two irregular vertices with $n_1 = 5$, $n_2 = 7$ with overlapping neighborhood before (top row) and after the correction (bottom row). For color images please refer to our website.

§5. Conclusion

We have given a detailed analysis for the techniques presented in [4]. The analysis allows to quantify the difference between the modified and unmodified surfaces and to deal with problems imposed by the topology of the initial control net. Furthermore, it is possible to apply the technique without using shape charts.

§6. Acknowledgments

References

1. U. Augsdörfer, N. A. Dodgson, and M. A. Sabin. Tuning subdivision by minimising the Gaussian curvature variation near extraordinary vertices. In E. Gröller and L. Szirmay-Kalos, editors, *Eurographics*, 2006.

2. L. Barthe and L. Kobbelt. Subdivision scheme tuning around extraordinary vertices. *Comput. Aided Geom. Design* 21(6) (2004), 561–583.

3. E. Catmull and J. Clark. Recursive generated b-spline surfaces on arbitrary topological meshes. *Computer-Aided Design*, 10 (1978), 350–355.

4. I. Ginkel and G. Umlauf. Loop subdivision with curvature control. In K. Polthier and A. Sheffer, editors, *Symposium on Geometry Processing*, 2006, 163–172.

5. I. Ginkel and G. Umlauf. Symmetry of shape charts, 2006. Submitted.

6. F. Holt. Towards a curvature continuous stationary subdivision algorithm. *Z. Angew. Math. Mech.* 76 (1996), 423–424.

7. C. Loop. Smooth subdivision surfaces based on triangles. Master's thesis, University of Utah, 1987.

8. C. Loop. Bounded curvature triangle mesh subdivision with the convex hull property. *The Visual Computer* 18 (2002), 316–325.

9. C. Loop. Smooth ternary subdivision of triangle meshes. In A. Cohen, J.-L. Merrien, and L.L. Schumaker, editors, *Curve and Surface Fitting – Saint-Malo 2002*, Nashboro Press (Brentwood), 2003, 295–302.

10. J. Peters and U. Reif. Shape characterization of subdivision surfaces - basic principles. *Comput. Aided Geom. Design* 21(6) (2004), 585–599.

11. H. Prautzsch and G. Umlauf. Improved triangular subdivision schemes. In F.-E. Wolter and N.M. Patrikalakis, editors, *Computer Graphics International 1998*, IEEE Computer Society, 1998, 626–632.

12. U. Reif and J. Peters. Structural analysis of subdivision surfaces - a summary. In K. Jetter, M. Buhmann, W. Haussmann, R. Schaback, and J. Stoeckler, editors, *Topics in Multivariate Approximation and Interpolation*, 2006, 149–190.

13. M.A. Sabin. Cubic recursive division with bounded curvature. In P.J. Laurent, A. Le Méhauté, and L.L. Schumaker, editors, *Curves and Surfaces*, 1991, 411–414.

Ingo Ginkel and Georg Umlauf
Geometric Algorithms Group
University of Kaiserslautern, Germany
{ginkel|umlauf}@informatik.uni-kl.de
http://www-umlauf.informatik.uni-kl.de